Journal Name

ARTICLE TYPE

Cite this: DOI: 00.0000/xxxxxxxxxx

Automated electrolyte formulation and coin cell assembly for high-throughput lithium-ion battery research

Jackie T. Yik,[a*] Leiting Zhang,[a*] Jens Sjölund,[b] Xu Hou,[a] Per H. Svensson[c,d], Kristina Edström,[a] and Erik J. Berg[a]

Received Date
Accepted Date

DOI: 00.0000/xxxxxxxxxx

Data-driven experimentation can accelerate battery research dramatically by closing the experimentation–analysis loop. Experimentation in traditional battery research is acknowledged to be heavily time-consuming and often suffers from large cell-to-cell variations. For closed-loop approaches, however, reliable and rapid performance evaluation is vital. Automation promises to enhance both the rate of testing and reproducibility. Herein, we present ODACell, an automated electrolyte formulation and battery assembly system, capable of preparing large batches of coin cells. We demonstrate the feasibility of Li-ion cell assembly in ambient atmosphere by preparing $LiFePO_4$ || $Li_4Ti_5O_{12}$ –based full cells with dimethyl sulfoxide–based model electrolyte. Furthermore, the influence of water is investigated to account for the hygroscopic nature of the non-aqueous electrolyte when exposed to ambient air. Reproducibility tests demonstrate a conservative fail rate of 5%, while the relative standard deviation of the discharge capacity after 10 cycles was 2% for the studied system. Electrolytes with 2 vol% and 4 vol% of water showed overlapping performance trends, highlighting the nontrivial relationship between water contaminants in electrolytes and cycling performance. Thus, reproducible data are essential to ascertain whether or not there are minor differences in performance for high-throughput electrolyte screenings. ODACell is broadly applicable to coin cell assembly with liquid electrolytes and therefore presents an essential step towards accelerating research and development of such systems.

Introduction

Global electrification powered by renewable energy sources requires next-generation batteries.[1] However, research and development of new battery chemistries are time-intensive tasks of arduous manual testing that can take decades from initial discovery to commercialization.[1] Therefore, acceleration of research and development is imperative to meet the growing demands. One contribution towards acceleration is automating the workflow. However, robotic setups have only been presented thus far for parts of the workflow, such as for the material discovery process with electrolyte formulations,[2,3] or just the battery cell assembly process with electrolyte dispensing.[4] We aim to present an automated setup that has integrated electrolyte formulation alongside battery assembly and electrolyte dispensing, automating the entire workflow.

A critical part of the battery research process is assembling and performance-testing battery cells. The electrochemical tests alone may take days, months or even years to complete.[5] Because of this manual effort and long testing duration, it is common to see data having only a few replicates. However, human error associated with electrolyte formulations, processing electrodes, and battery assembly give rise to battery performance variations. In order to rely on the results, cell-to-cell variability must be overcome through rigorous reproducibility verification of the data. A study by Dechent *et al.*[6] suggested a minimum of 9 replicates to be able to fit a battery aging model with one parameter. The complexity of the system strongly affects the number of replicates required to provide reliable results that can decouple the various effects and reactions in the system.

Moreover, conventional strategies for battery material discoveries rely heavily on "trial-and-error" approaches, where each subsequent step of the discovery process is dependent on the successful completion of the previous step.[1] State-of-the-art strategies have shifted towards a "closed-loop" approach, where all completed steps inform and predict the following steps, eliminating the sequential dependence.[1,7–9] For new material discoveries,

[a] *Department of Chemistry - Ångström Laboratory, Uppsala University, P.O. Box 538, SE-751 21 Uppsala, Sweden. Email: jackie.yik@kemi.uu.se, leiting.zhang@kemi.uu.se*
[b] *Department of Information Technology, Uppsala University, P.O. Box 337, SE-751 05 Uppsala, Sweden*
[c] *Chemical and Pharmaceutical Development, RISE Research Institutes of Sweden, SE-151 36, Södertälje, Sweden*
[d] *Applied Physical Chemistry, Department of Chemistry, KTH Royal Institute of Technology, SE-114 28, Stockholm, Sweden*

closed-loop experiments can optimize material selection within a design space quickly, discovering the optimum faster than conventional trial-and-error procedures and with fewer experiments.[10]

While closed-loop approaches utilize previous experiments, high-throughput experiments are often used alongside these approaches to build a library of results needed for the optimization inputs. Methods that allow automatic measurements of a defined design subspace at a high rate are considered high-throughput.[11] For example, Yang *et al.*[12] used high-throughput optical measurements to identify regions in three-cation metal oxide composition spaces whose optical trends were not simple phase mixtures, while McCalla *et al.*[13] demonstrated a workflow capable of collecting hundreds of x-ray diffraction patterns and electrochemical impedance spectroscopy spectra, simultaneously, per week.

Herein, we present ODACell, an automated robotic setup capable of electrolyte formulation, coin cell assembly, and electrochemical testing. By automating these three tasks, human error can be reduced, and the experimentation process can be accelerated. Demonstrating the capabilities of a relatively simple and affordable robotic setup is promising for the transition of small batch upscaling in academic research and progression of data-driven studies.[4,14]

Zhang *et al.*[4] recently presented their automated setup, AutoBASS, for one of the steps in the workflow: coin cell assembly. While automating the assembly process removes an arduous task where mistakes can be made, their robotic setup remains to be positioned for transition into closed-loop experimentation. Although assembling coin cells and electrolyte dispensing are automated, electrolytes would still need to be prepared manually. Conversely, our robotic setup has electrolyte formulation capabilities in addition to coin cell assembly and electrolyte dispensing. With this, not only automation, but autonomous, closed-loop experimentation is possible. Other robotic setups exist but are mainly targeted towards material characterization such as for the ionic conductivity of electrolyte fomulations[3,14] or optical and electronic properties of thin-film materials.[15] Besides AutoBASS, to our knowledge no other published automated robotic setups for coin cell assembly and electrolyte dispensing has been presented thus far.

In this work, we describe an automated robotic setup for electrolyte formulation, assembly and cycling of coin-type battery cells in an ambient laboratory environment. Working in an ambient atmosphere is substantially more cost-effective than maintaining a dry room for cell assembly, potentially opening up the underexplored electrolyte design space with battery materials tolerating ambient atmosphere. Our affordable and flexible setup can be adapted to different systems (e.g. non-aqueous electrolytes) with minor modifications; the addition or removal of hardware components can easily be integrated while maintaining, adjusting, or enhancing functionality, characterizing ODACell as a modular setup. The possibility to use ODACell for diverse chemistries generalizes its applicability to explore the high research potential of liquid electrolytes, which have continued to be a challenge to optimize owing to the vast design space.[9] The modular setup thus has an advantage over static robotic research setups. To this end, the objectives of this work are to (1) design and construct an affordable, modular battery assembly and testing setup with electrolyte formulation and dispensing ability, (2) determine the cell-to-cell variability and reproducibility of the system for cells assembled in ambient atmosphere, and (3) demonstrate the setup's practical applicability by preparing and performance-testing hybrid electrolytes containing mixtures of binary solvents, namely water and dimethyl sulfoxide in a full cell configuration.

Methods

Robotic Assembly and Electrolyte Formulation

The robotic setup, ODACell, is shown in Figure 1A, consisting of three 4-axis robotic arms (Dobot MG400, China) and one liquid handling robot (Opentrons OT-2, USA, Figure 1B). Each robotic arm was equipped with a unique head for specialized function (Figure 1C). A custom-made vacuum head holder with two vacuum saving valves (SMC ZP2V, Japan) was set up on one robot allowing it to pick up components; a custom-made claw head and matching holder allowed one robot to collect and move the component stack; and one robot was equipped with an electric gripper (DBT-PGS5, China). A modified electric coin cell crimper (TMAX, China) was connected to interface with the robotic arms, and all robots were fixed to the tabletop. An elevated platform was installed on the tabletop. The platform was used to place custom-made coin cell component trays and holders for battery cycling. Each tray contained enough components for four coin cells and multiple trays were loaded in stacks.

Orchestration of the electrolyte formulation and cell assembly process was done in Python. The full code and data can be found in Github.* Python integration was included with the software development kits of the liquid handling robot and robotic arms. Low-level proprietary functions were wrapped together to form custom, specialized high-level functions for each robot. Commands execute the high-level functions sequentially via position triggers to perform specific tasks.

Material Selection and Preparation

$LiFePO_4$ (lithium iron phosphate, LFP) cathode and $Li_4Ti_5O_{12}$ (lithium titanate, LTO) anode were selected for their known structural and cycling stability[16,17] as well as their commercial availability. Considering the focus of this study was on the robotic setup and reproducibility, commercial electrodes provide highly reliability mass loading, eliminating a potential source of error. A dimethyl sulfoxide (DMSO, $(CH_3)_2SO$)–based electrolyte was selected because of its environmental sustainability[18] and potential for high-voltage applications.[19]

CR2025 coin cell parts (316 stainless steel) were used as received. LFP cathode and LTO anode sheets were ordered from CustomCells, Germany. The manufacturer specified specific capacity was 150 mAh g^{-1} for both cathode and anode sheets. Cathode and anode with 16 mm and 13 mm respective diameters were used. Separators (GF/A glass fiber, GE Healthcare) were 18 mm diameter. Electrodes and separators were prepared in ambient

* https://github.com/jyik/ODACell

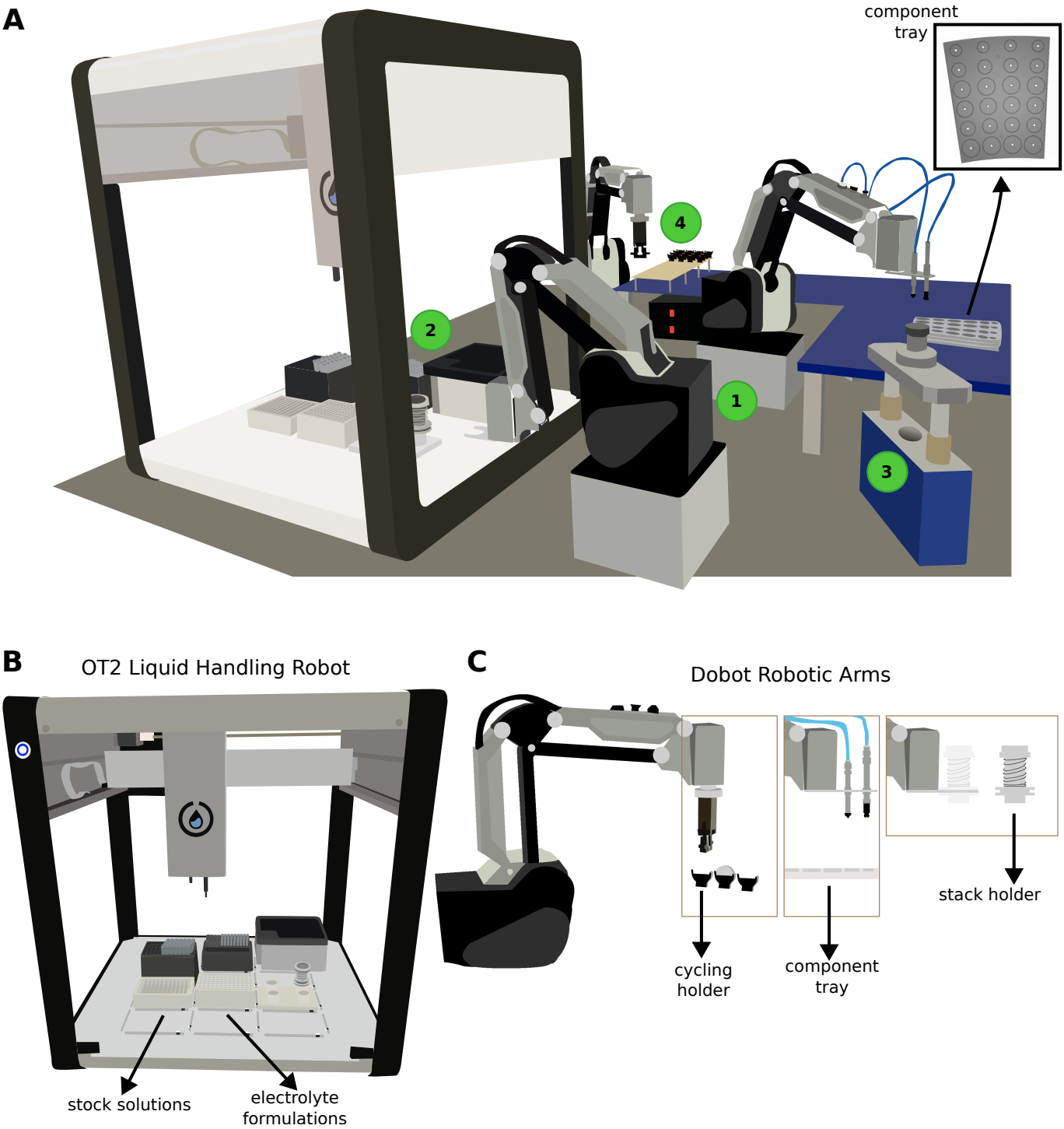

Fig. 1 Schematic illustration of the automated robotic assembly setup. (A) The four robots (three 4-axis robotic arms and one liquid handling robot) are detailed along with the elevated platform where the battery cycling station and coin cell components are placed. Numbered circles are placed at key positions in the assembly process: (1) placing coin cell components, (2) acquiring electrolyte, (3) crimping, and (4) cycling the coin cell. (B) The liquid handling robot where electrolyte formulation occurs. Stock solutions are loaded into the reservoirs and the robot can mix them together in the adjacent wells to formulate different electrolyte compositions. (C) The three 4-axis robotic arms handling the coin cell assembly and battery cycling. Each one has its own unique attachments to perform specific tasks.

atmosphere as well as handling of all coin cell components.

Two electrolyte stock solutions were prepared. Lithium perchlorate ($LiClO_4$) (99.99%, battery grade) and Dimethyl sulfoxide (DMSO, $(CH_3)_2SO$) (anhydrous, $\geq$99.9%) were obtained from Sigma Aldrich. Milli-Q water was obtained from SPEX CertiPrep (Assurance® grade, Type I water). Batches of 2 mol kg^{-1} (molality, m) $LiClO_4$ in DMSO and 2 m $LiClO_4$ in water electrolyte stock solutions were prepared prior to coin cell assembly. 2 m $LiClO_4$ in DMSO stock solutions were stored under inert atmosphere and transferred into ambient atmosphere just before assembling a batch of coin cells. 2 m $LiClO_4$ in water stock solutions were prepared by mixing $LiClO_4$ salt with water just before assembling a batch of coin cells.

Experimentation

To evaluate the cell-to-cell variability and assembly reproducibility, 83 cells were assembled in six batches (3 cells in the first batch, 16 cells per batch thereafter) using 2 m $LiClO_4$ in DMSO electrolyte.

To systematically explore the influence of water in the electrolyte, galvanostatic cycling performance of LFP || LTO full cells with electrolytes containing mixtures of water in DMSO were compared. The first hybrid electrolyte was prepared by mixing 840 µL of 2 m $LiClO_4$ in DMSO and 160 µL of 2 m $LiClO_4$ in water. Mixing was done by aspirating and dispensing 700 µL of the mixture 20 times. The next hybrid electrolyte composed of 500 µL from the previous mixture and 500 µL from the 2 m $LiClO_4$ in DMSO stock solution using the same mixing procedure. The same operations for the third and fourth hybrid electrolytes were done, producing 16 vol%, 8 vol%, 4 vol%, and 2 vol% H_2O–electrolytes. 12 coin cells were assembled and cycled for each hybrid electrolyte. One electrolyte formulation was mixed, then a batch of coin cells were assembled; this process was repeated for the four hybrid electrolytes.

Cycling Procedure

Galvanostatic cycling was performed using a battery cycler with 16 total channels from Astrol Electronic AG, Switzerland. Since the cathode was oversized, recorded capacity was normalized with respect to the LTO active mass. The mean LTO active mass (8.84 mg) was used for all cells. The cycling procedure had a rest period of 2 hours for wetting. Charging and discharging cycles followed for 10 cycles using a constant C/2 rate (1C = 150 mA g^{-1}) translating to a constant current (CC) of 0.663 mA. The charging and discharging CC step was between the voltage range of 1.6 to 2.2 V.

Results and Discussion

ODACell Setup

The coin cell assembly process was as follows: a robotic arm equipped with a vacuum head loaded the positive casing, followed by the cathode, then separator onto a holder attached to another robotic arm (location 1 in Figure 1A); the holder was then moved into the liquid handling robot and 45 µL of the desired electrolyte was dispensed (location 2 in Figure 1A); the holder then returned to the previous position to receive the anode, spacer and spring, and the negative casing with gasket, sequentially (location 1 in Figure 1A); upon placement of the negative casing, the robotic arm with the vacuum head applied a downward force on the stack to ensure flush closure of the cell; the holder with all the components entered the crimper to seal the coin cell (location 3 in Figure 1A); the crimped coin cell was delivered to the cycling station by the robotic arm with the vacuum head, where another robotic arm with a gripper loaded the cell into an empty holder for galvanostatic cycling (location 4 in Figure 1A).

Based on the current cycling protocol, one cell takes *ca.* 42 hours to collect a data sample, of which 4 minutes is from assembling the cell as described in the previous paragraph. Therefore, the current bottleneck is the battery cell cycling step. Currently, with 16 cycling channels, the setup is not capable of continuous assembly. Consequently, the number of channels in the setup will determine the bottleneck. We will soon increase the number of channels to 200 and then a 13 hour cycling protocol would enable continuous assembly and testing (where automated electrolyte formulation is done independently of assembly, achieved by parallelizing the orchestration). Depending on the desired battery evaluation procedure, a 13 hour cycling protocol is feasible. The choice of 10 cycles for this work was to be able to observe and compare the performance trends of the cells containing different hybrid electrolytes in the water concentration series experiments; and the choice of 2 hours rest period for wetting and C/2 cycling rate was not optimized in this work. Increasing the number of channels and decreasing the cycling time will reduce bottlenecks in the system to achieve higher throughput.

In the case of systems-level applications, such as assembling and cycling battery cells, the throughput is intrinsically lower compared to material-level applications. Stein *et al.* [20] provided a conceptual summary visualizing different throughputs of acceleration setups on a materials-interfaces-systems scale. While setups developed for characterization of materials and interfaces can acquire data within seconds,[3,12,20,21] testing an assembled cell may take months. The definition of high-throughput, therefore, can change depending on the application. For systems-level setups, a different approach on throughput can be considered that focuses on the initial experiment and continuous experimentation separately. If the assembling time for a batch and the testing time for each cell is the same as described earlier, then the throughput for data acquisition is limited by the assembly time. That is to say, for assembling and testing cells, the first cell will take the longest time to acquire data, but the subsequent cells will take much shorter time, assuming finished cells are continuously replaced with new cells. Failed cells and other complications may arise in the assembly or testing processes, but the average throughput should be consistent. ODACell is a step towards high-throughput and as such intended to demonstrate how the setup can be used for intelligent exploratory screening with high repeatability and analytical capabilities to detect novel candidate electrolyte systems.

Comparison of the presented setup to other systems developed by other groups is limited owing to the lack of publicly published

setups. Commercially available robotic setups, such as the one optimized for battery applications,[22] on the other hand, are not easily modified and have limited possibility for advancement, making it hard to adjust and customize any of the hardware and software. With publicly publishable setups, such as ODACell, a modular system can be made, where any addition of robots or changes in software can be implemented and orchestrated together. Conversely, static setups, such as Clio,[3] control specific machinery, such as pumps and valves. Comparing ODACell to AutoBASS[4], another systems-level automated setup, ODACell has the ability to formulate electrolytes in additional to coin cell assembly and electrolyte dispensing which AutoBASS is limited to. AutoBASS has a camera to monitor the component placement, which will be included in ODACell as well. AutoBASS has one less robotic arm than ODACell making it more space efficient but also removing any potential flexibility an additional robotic arm would provide. ODACell's addition of a liquid handling robot along with a robotic arm allows more of the material discovery workflow (e.g. electrolyte discovery process) to be automated compared to AutoBASS. Another robotic setup from the Research Institute of Sweden (RISE), Poseidon, has been developed that is capable of electrolyte formulation, Raman spectroscopic characterization, and cycling evaluation, but lack batch assembly capabilities owing to only having a single robotic arm.

Reproducibility

Figure 2 shows the distribution of the cycle 1, 2, and 10 discharge capacities along with the cycling performance for cycle 10. For the distribution shown in Figure 2A, the mean and standard error for cycles 1, 2, and 10 are 149.8 $\pm$ 0.3 mAh g^{-1}, 146.4 $\pm$ 0.3 mAh g^{-1}, and 135.1 $\pm$ 0.3 mAh g^{-1}, respectively. For cycle 10, the standard error translates to 3.0 mAh g^{-1} or 2.1% standard deviation for sampled data around the mean. The distribution is negatively skewed (Fisher-Pearson coefficient of skewness $=$ -0.34 for cycle 1) and lacks an overt shape. In contrast, Gaussian distributions are seen in the discharge capacities of the cells from the robotic assembly setup by Zhang *et al.*[4] However, the different systems may partially explain the discrepancy. In non-aqueous systems, the assembly process must be done under inert atmosphere because of the reactivity of the electrolyte with moisture. In contrast, the selected chemistry of our system is more tolerant to air and moisture, but still experience side reactions, as the Coulombic efficiency is less than 100%. The longer the electrolyte is exposed to the environment, the higher the risk that O_2 and H_2O adversely influence cell performance.[23] Future updates to ODACell will include an automated vial de-/capping accessory. Important to note, no electrode passivation layers (e.g. solid electrolyte interphase) are known to form in our system.[24]

Misalignment of components and electrical contact issues were the main sources of error. Although the robotic arm's vacuum head drop placement was centered in the holder, the cathode or separator could still slightly deviate from center position due to the separator being dropped onto the curved cathode surface. Dropping the spacer and spring on the stack could also shift the weight of the stack causing misalignment. Small variations in the electrodes' mass loading will also influence the performance distribution but its effect was minimized by using commercial electrodes (active material mass standard deviation *ca.* 5%) instead of inhouse-made electrodes (active material mass standard deviation *ca.* 20%). Commercial electrodes are manufactured to have reliable specified capacity whereas inhouse-made electrodes could have wide variations depending on the slurry coating process. Another factor influencing the distribution is exposure of the electrolyte to air before assembly. As discussed in the previous paragraph, the current setup has the electrolyte open during assembly. The electrolyte is hygroscopic so water is gradually absorbed into the electrolyte; however, exposure to air was limited by storing the electrolyte under inert atmosphere until use and making fresh stock electrolyte for each batch. Exposure of electrolyte to the ambient atmosphere ranged from 5 minutes for the first cell assembled in a batch to 45 minutes for the last cell in a batch. To reduce any performance deviations due to contamination of suction cups, two vacuum heads were deployed; one contacting components related to the anode, and one to the cathode, thereby reducing the risk of cross-contamination. Additionally, a chemically inert (polyether ether ketone, PEEK) vacuum head insert was attach to the suction cup coming in direct contact with the porous cathode material surface.

Figures 2B and 2C show different representations of the charge and discharge curves for cycle 10, where areas with similarly performing cells overlap and have higher saturation of color. From Figure 2C, there is some variation where the plateau occurs, and there is one cell experiencing contact issues represented by the extra peak in the discharge differential capacity curve. The standard error throughout the cycles remained 0.3 mAh g^{-1}, and the higher sample size translates to a smaller standard error. However, in practice, 80 replicates is infeasible and a more realistic goal is 12 replicates, which is demonstrated with the water concentration series.

Water Concentration Series

A further motivation for the water concentration series experiments, besides systematically exploring the influence of water in the electrolyte due to air exposure, is to demonstrate the entire automated workflow for electrolyte discovery, from electrolyte formulation to performance testing, in a practical application. Figure 3 shows the galvanostatic cycling data for cells with electrolytes containing variable amounts of added water. The cells used to determine reproducibility are used for the 0 vol% H_2O–electrolyte group. In Figure 3A and 3B, the mean capacities decrease with increasing water content. The trend is consistent throughout the 10 cycles. The performance between 4 vol%, 2 vol%, and 0% H_2O–electrolyte groups are, however, indistinguishable from each other; the mean discharge capacities for cycle 10 were 120.6 $\pm$ 5.7 mAh g^{-1}, 133.0 $\pm$ 0.7 mAh g^{-1}, 135.3 $\pm$ 0.6 mAh g^{-1}, 135.3 $\pm$ 0.6 mAh g^{-1}, and 135.3 $\pm$ 0.3 mAh g^{-1} for the 16 vol%, 8 vol%, 4 vol%, 2 vol%, and 0% H_2O–electrolyte groups, respectively.

The Coulombic efficiency for the different water content electrolytes in Figure 3C show that the 16 vol% H_2O–electrolyte

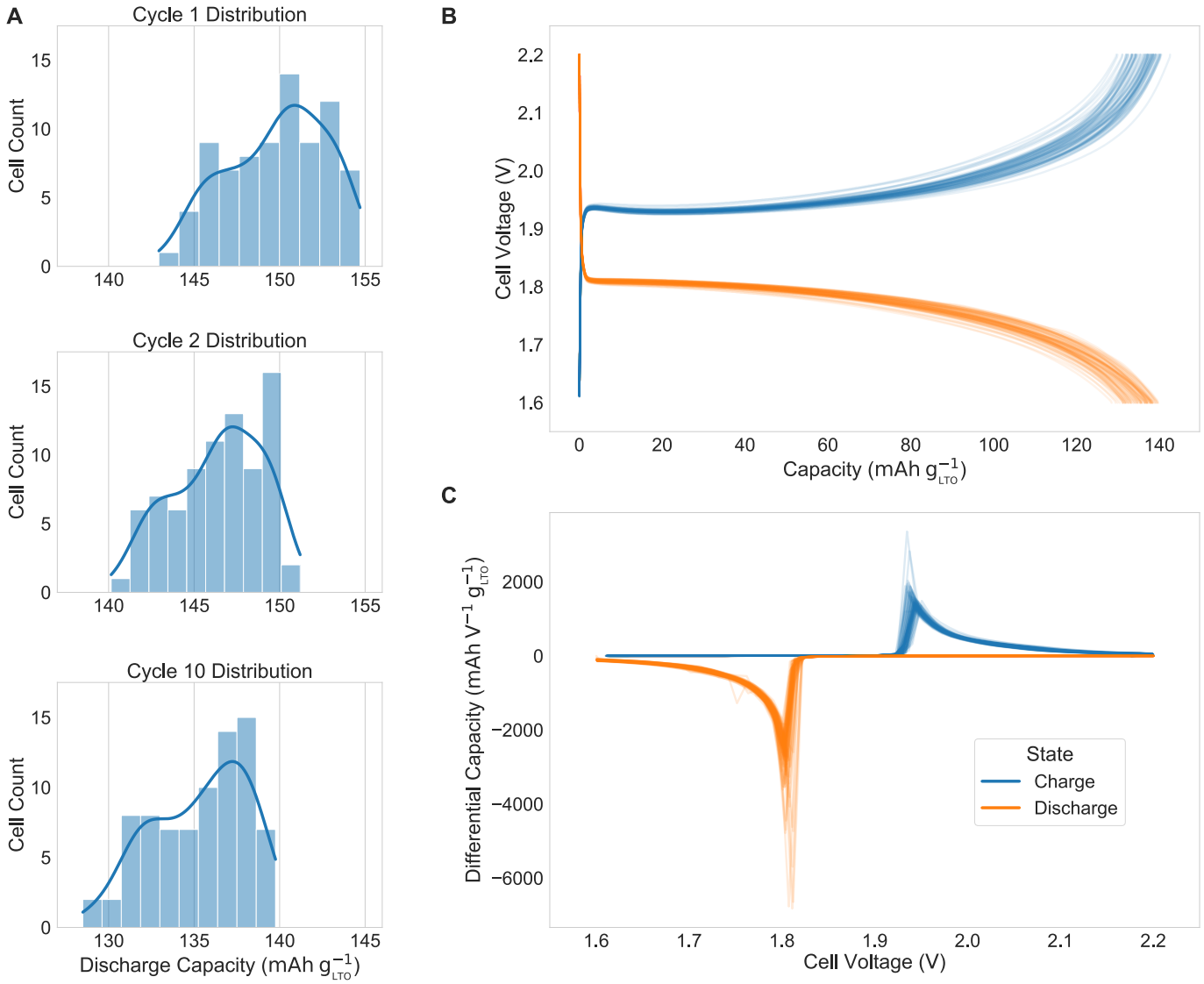

Fig. 2 Distribution and cycling performance of the 80 coin cells assembled by the automated robotic setup. (A) Variation of the discharge capacities for cycle 1, 2, and 10. The mean and standard error for cycles 1, 2, and 10 are 149.8 ± 0.3 mAh g^{-1}, 146.4 ± 0.3 mAh g^{-1}, and 135.3 ± 0.3 mAh g^{-1}, respectively. (B) Charge and discharge curves for cycle 10 of the 80 coin cells. The denser the lines, the bolder the color. (C) Cycle 10 differential capacity of the 80 coin cells computed by resampling the curves from (B). The denser the lines, the bolder the color. Error bars are standard error.

group is consistently lower compared to the other three dilution groups throughout the 10 cycles. The 8 vol%, 4 vol%, 2 vol%, and 0% H_2O–electrolyte cells have similar Coulombic efficiencies (99.0 ± 0.2 %, 99.4 ± 0.1 %, 98.9 ± 0.2 %, 99.3 ± 0.1 % respectively for cycle 10). Side reactions involving water are driving the capacity and efficiency trends.

Performance trends between the different hybrid electrolytes are largely due to the water content in the system. Increasing the amount of water increases the prevalence of water reduction due to the narrow stability window of water (1.23 V). DMSO, however, can suppress interfacial electrochemical reactions of water molecules by entering the cation solvation sheath directly and form DMSO–H_2O H-bond networks that effectively reduce the activity of water molecules.[25] The H-bond structure in the solution affects the water reduction reaction so small amounts of water in the DMSO hybrid electrolyte is tolerable and water reduction can be largely suppressed. With increased amounts of water, the DMSO–H_2O H-bond network is less prevalent, becoming unable to effectively suppress the water reduction reaction. Consequently, small amounts of gas from water reduction can cause increased internal impedance from mechanical disintegration of the electrodes or other side reactions due to local pH changes at the electrodes.[23] Water reduction likely explains the lower Coulombic efficiencies and capacities evident from the trends of Figure 3. Nevertheless, the 2 vol% and 4 vol% H_2O–electrolyte cells have similar capacities after 10 cycles as these concentrations of water are insufficient to significantly affect cell performance. The relationship between capacity drop and water content is not trivial. However, differences between the hybrid electrolytes and any possible outliers would become more evident with more cycles.

The charge/discharge curves of Figure 4A reveal two possible outliers (also seen in Figure 4B appearing shallower and having

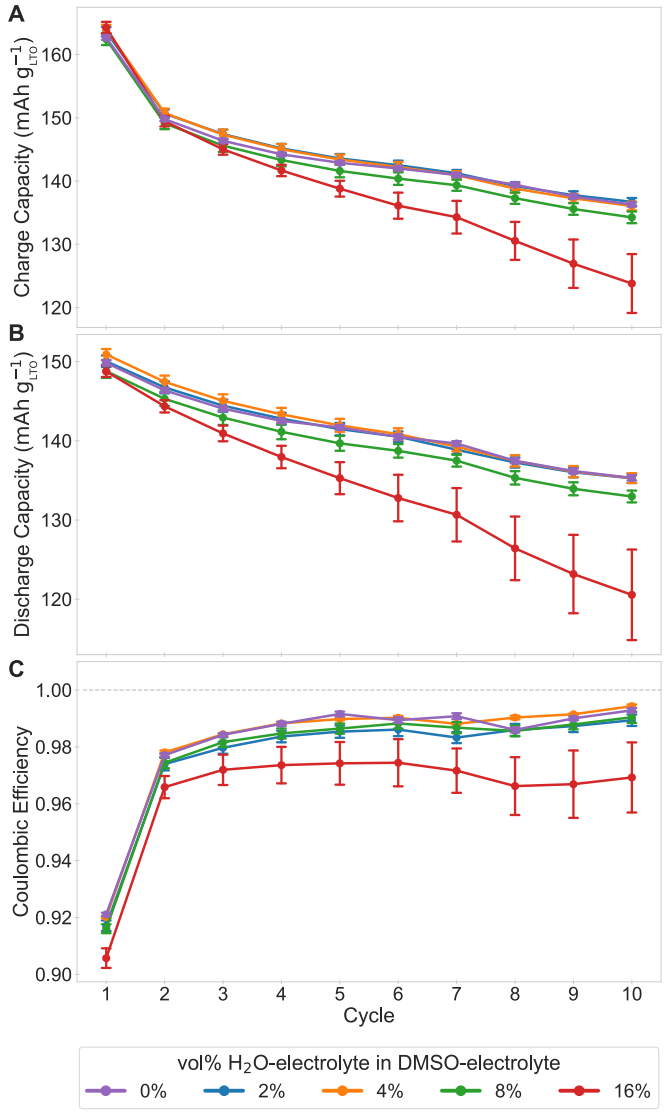

Fig. 3 Specific capacity and energy trends with different volume percent of H_2O – electrolyte in dimethyl sulfoxide (DMSO) – electrolyte. Error bars are standard error. (A, B) Charge and discharge specific capacity normalized to the mean anode active material (lithium titanate, LTO) vs cycle, (C) Coulombic efficiency computed from (A) and (B) vs cycle.

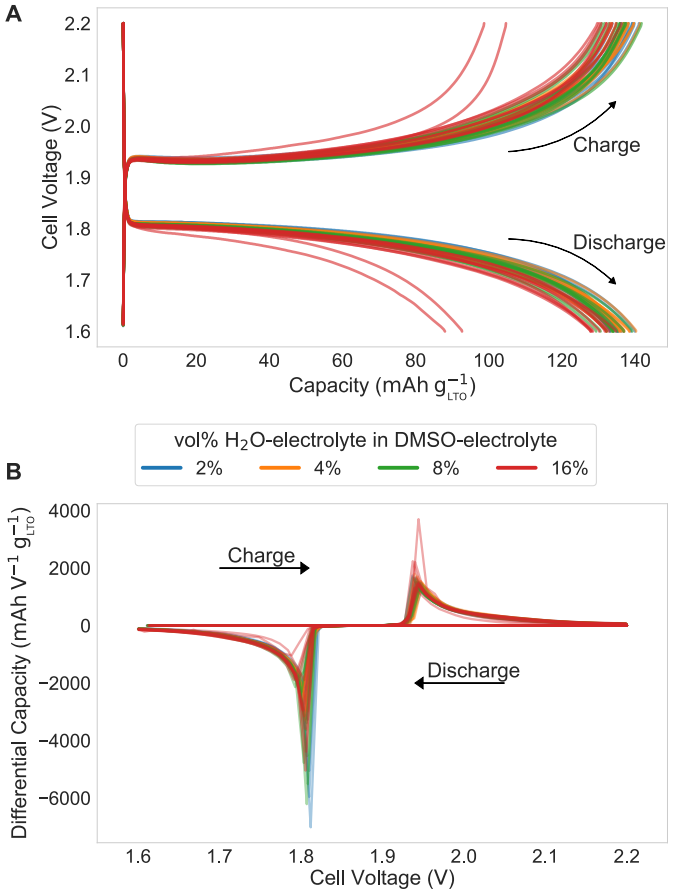

Fig. 4 Distribution of assembled coin cells with varying water content in electrolyte for cycle 10. (A) Charge and discharge curves for cycle 10. Two possible outliers are seen. (B) Differential capacity of the curves in (A). The two outliers are harder to visualize.

slightly shifted peaks). These two cells both belong to the 16 vol% H_2O–electrolyte group and exhibited faster capacity fade compared to the other cells in the group. These two cells contribute to the increased variance for the group (visualized by larger error bars in Figure 3). If the two outliers were removed from the analysis, the relative standard deviation would decrease from 15.7% (standard error 5.7 mAh g^{-1}) to 2.4% (standard error 1.0 mAh g^{-1}). The increased capacity fading could be attributed to the electrolyte mixing process. If the two stock solutions were not sufficiently mixed, the resulting electrolyte solution would not be homogenous and, subsequently, cells could receive electrolyte containing varying water content. We will optimize electrolyte mixing protocols to minimize the impact of insufficient mixing.

Overall, the water concentration series demonstrates that the DMSO–based electrolyte can tolerate up to 4% of water in its formulation without observable performance degradation within 10 cycles and reinforces the necessity of replicates in practice. Presence of side reactions can cause wider variation in the data; therefore, more complex systems may require more replicates to have observable effects on performance. The relative standard deviation was 1.4%, 1.6%, 1.9%, and 15.7% for 2, 4, 8, and 16 vol% H_2O–electrolyte cells, respectively. Since the variance of the discharge capacity with little water content (2, 4, and 8 vol% in the water concentration series) in the electrolyte is similar to the electrolyte without any added water, 12 replicates to evaluate reproducibility, instead of 80 replicates, would have sufficed. Although the current robotic setup may suffer from the open system of the electrolyte formulation step, it is a methodology that can handle future high-throughput tests and closed-loop exploration of the electrolyte design space. There already exists frameworks for combining automation and machine learning to achieve autonomous setups in different applications.[26,27] In future work, we will adapt a framework and incorporate an optimization algorithm, such as a Bayesian optimizer, e.g. to evaluate the influence of oxygen scavengers and other electrolyte additives in aqueous lithium-ion batteries.[28] In addition to building upon the current setup, improvements to this setup could further increase reproducibility and reduce variance between the performance of cells.

We have planned to introduce a camera system as well as position calibration for the setup, ensuring proper placement of assembly components. Furthermore, as previously discussed, we plan on designing an apparatus to store electrolytes in a closed system to reduce extended periods of exposure to ambient atmosphere.

Conclusions

In this work, the capabilities of ODACell, an automated robotic coin cell assembly and electrolyte formulation setup was demonstrated. A conservative estimate of the assembly failure rate for the current setup is 5% from the 131 coin cells assembled for this work. Component misalignment causing short-circuits and electrical contact issues were the main sources of failure. The relative standard deviation of cycle 10's discharge capacity was 2% for our system. The proposed improvements would improve the variability of the cells assembled making the setup reliable and affordable for research of electrolytes compatible with the ambient laboratory atmosphere.

We demonstrated the seamless integration of a liquid handling robot into the assembly setup and tested different water contents in the electrolyte. Automating the entire workflow and having a modular setup distinguish our setup from others. With the electrolyte formulations made by the liquid handling robot, consistent and reproducible performance metrics between the formulations were observed. Noticeably, there was little difference in capacity and Coulombic efficiency between 4 vol%, 2 vol%, and 0% H_2O–electrolyte cells, suggesting a nontrivial relationship of electrolytes containing mixtures of small amounts of water in DMSO. The water concentration series experiment demonstrates the tolerance of DMSO–based electrolytes to minor amounts (up to 4%) of water in its formulation without significant detriment to the performance of batteries. This is necessary if lithium-ion batteries are to be assembled under ambient conditions. Dry rooms are expensive in terms of cost and energy. Moreover, this reinforces the need for more replicates when exploring different liquid electrolyte compositions in order to accurately determine trends and optimize liquid electrolyte design. The electrolyte evaluated herein may form a basis for further exploration of water-tolerable electrolyte for higher voltage Li-ion batteries.

Author Contributions

Jackie T. Yik: Investigation, Software, Formal analysis, Writing - Original Draft, Writing - Review & Editing, Visualization. **Leiting Zhang:** Methodology, Conceptualization, Resources, Writing - Review & Editing, Supervision. **Jens Sjölund:** Resources, Writing - Review & Editing, Supervision. **Xu Hou:** Resources, Writing - Review & Editing. **Per H. Svensson:** Writing - Review & Editing. **Kristina Edström:** Conceptualization, Project administration, Funding acquisition. **Erik J. Berg:** Methodology, Conceptualization, Resources, Writing - Review & Editing, Supervision, Funding acquisition, Project administration.

Conflicts of interest

There are no conflicts to declare.

Acknowledgements

This research was financially supported by the Swedish Energy Agency (Grant 50119-1), Stiftelsen för Strategisk Forskning (SSF, FFL18-0269), Knut and Alice Wallenberg (KAW) Foundation (Grant 2017.0204) and StandUp for Energy for base funding. This research was also supported by Wallenberg AI, Autonomous Systems and Software Program (WASP) funded by the KAW Foundation.

References

1 J. Amici, P. Asinari, E. Ayerbe, P. Barboux, P. Bayle-Guillemaud, R. J. Behm, M. Berecibar, E. Berg, A. Bhowmik, S. Bodoardo, I. E. Castelli, I. Cekic-Laskovic, R. Christensen, S. Clark, R. Diehm, R. Dominko, M. Fichtner, A. A. Franco, A. Grimaud, N. Guillet, M. Hahlin, S. Hartmann, V. Heiries, K. Hermansson, A. Heuer, S. Jana, L. Jabbour, J. Kallo, A. Latz, H. Lorrmann, O. M. Løvvik, S. Lyonnard, M. Meeus, E. Paillard, S. Perraud, T. Placke, C. Punckt, O. Raccurt, J. Ruhland, E. Sheridan, H. Stein, J.-M. Tarascon, V. Trapp, T. Vegge, M. Weil, W. Wenzel, M. Winter, A. Wolf and K. Edström, A Roadmap for Transforming Research to Invent the Batteries of the Future Designed within the European Large Scale Research Initiative BATTERY 2030+, *Advanced Energy Materials*, 2022, **12**, 2102785.

2 A. Dave, J. Mitchell, K. Kandasamy, H. Wang, S. Burke, B. Paria, B. Póczos, J. Whitacre and V. Viswanathan, Autonomous Discovery of Battery Electrolytes with Robotic Experimentation and Machine Learning, *Cell Reports Physical Science*, 2020, **1**, 100264.

3 A. Dave, J. Mitchell, S. Burke, H. Lin, J. Whitacre and V. Viswanathan, Autonomous optimization of non-aqueous Li-ion battery electrolytes via robotic experimentation and machine learning coupling, *Nature Communications*, 2022, **13**, 5454.

4 B. Zhang, L. Merker, A. Sanin and H. S. Stein, Robotic cell assembly to accelerate battery research, *Digital Discovery*, 2022, **1**, 755–762.

5 J. E. Harlow, X. Ma, J. Li, E. Logan, Y. Liu, N. Zhang, L. Ma, S. L. Glazier, M. M. E. Cormier, M. Genovese, S. Buteau, A. Cameron, J. E. Stark and J. R. Dahn, A Wide Range of Testing Results on an Excellent Lithium-Ion Cell Chemistry to be used as Benchmarks for New Battery Technologies, *Journal of The Electrochemical Society*, 2019, **166**, A3031–A3044.

6 P. Dechent, S. Greenbank, F. Hildenbrand, S. Jbabdi, D. U. Sauer and D. A. Howey, Estimation of Li-Ion Degradation Test Sample Sizes Required to Understand Cell-to-Cell Variability**, *Batteries & Supercaps*, 2021, **4**, 1821–1829.

7 P. M. Attia, A. Grover, N. Jin, K. A. Severson, T. M. Markov, Y.-H. Liao, M. H. Chen, B. Cheong, N. Perkins, Z. Yang, P. K. Herring, M. Aykol, S. J. Harris, R. D. Braatz, S. Ermon and W. C. Chueh, Closed-loop optimization of fast-charging protocols for batteries with machine learning, *Nature*, 2020, **578**, 397–402.

8 M. Fichtner, K. Edström, E. Ayerbe, M. Berecibar, A. Bhowmik, I. E. Castelli, S. Clark, R. Dominko, M. Erakca, A. A. Franco,

A. Grimaud, B. Horstmann, A. Latz, H. Lorrmann, M. Meeus, R. Narayan, F. Pammer, J. Ruhland, H. Stein, T. Vegge and M. Weil, Rechargeable Batteries of the Future—The State of the Art from a BATTERY 2030+ Perspective, *Advanced Energy Materials*, 2022, **12**, 2102904.

9 A. Benayad, D. Diddens, A. Heuer, A. N. Krishnamoorthy, M. Maiti, F. L. Cras, M. Legallais, F. Rahmanian, Y. Shin, H. Stein, M. Winter, C. Wölke, P. Yan and I. Cekic-Laskovic, High-Throughput Experimentation and Computational Freeway Lanes for Accelerated Battery Electrolyte and Interface Development Research, *Advanced Energy Materials*, 2022, **12**, 2102678.

10 T. Lombardo, M. Duquesnoy, H. El-Bouysidy, F. Årén, A. Gallo-Bueno, P. B. Jørgensen, A. Bhowmik, A. Demortière, E. Ayerbe, F. Alcaide, M. Reynaud, J. Carrasco, A. Grimaud, C. Zhang, T. Vegge, P. Johansson and A. A. Franco, Artificial Intelligence Applied to Battery Research: Hype or Reality?, *Chemical Reviews*, 2022, **122**, 10899–10969.

11 A. Ludwig, Discovery of new materials using combinatorial synthesis and high-throughput characterization of thin-film materials libraries combined with computational methods, *npj Computational Materials*, 2019, **5**, 70.

12 L. Yang, J. A. Haber, Z. Armstrong, S. J. Yang, K. Kan, L. Zhou, M. H. Richter, C. Roat, N. Wagner, M. Coram, M. Berndl, P. Riley and J. M. Gregoire, Discovery of complex oxides via automated experiments and data science, *Proceedings of the National Academy of Sciences*, 2021, **118**, e2106042118.

13 E. McCalla, M. Parmaklis, S. Rehman, E. Anderson, S. Jia, A. Hebert, K. Potts, A. Jonderian, T. Adhikari and M. Adamič, Combinatorial methods in advanced battery materials design, *Canadian Journal of Chemistry*, 2022, **100**, 132–143.

14 A. Narayanan Krishnamoorthy, C. Wölke, D. Diddens, M. Maiti, Y. Mabrouk, P. Yan, M. Grünebaum, M. Winter, A. Heuer and I. Cekic-Laskovic, Data-Driven Analysis of High-Throughput Experiments on Liquid Battery Electrolyte Formulations: Unraveling the Impact of Composition on Conductivity**, *Chemistry–Methods*, 2022, **2**, e202200008.

15 B. P. MacLeod, F. G. L. Parlane, T. D. Morrissey, F. Häse, L. M. Roch, K. E. Dettelbach, R. Moreira, L. P. E. Yunker, M. B. Rooney, J. R. Deeth, V. Lai, G. J. Ng, H. Situ, R. H. Zhang, M. S. Elliott, T. H. Haley, D. J. Dvorak, A. Aspuru-Guzik, J. E. Hein and C. P. Berlinguette, Self-driving laboratory for accelerated discovery of thin-film materials, *Science Advances*, 2020, **6**, eaaz8867.

16 Y. Wang, P. He and H. Zhou, Olivine $LiFePO_4$: development and future, *Energy Environ. Sci.*, 2011, **4**, 805–817.

17 C. P. Sandhya, B. John and C. Gouri, Lithium titanate as anode material for lithium-ion cells: a review, *Ionics*, 2014, **20**, 601–620.

18 M. Wang, X. Dong, I. C. Escobar and Y.-T. Cheng, Lithium Ion Battery Electrodes Made Using Dimethyl Sulfoxide (DMSO)—A Green Solvent, *ACS Sustainable Chemistry & Engineering*, 2020, **8**, 11046–11051.

19 D. Wu, W. Y. Zhang, H. J. Feng, Z. J. Zhang, X. Y. Chen and P. Cui, Mechanistic Insights into the Intermolecular Interaction and Li^+ Solvation Structure in Small-Molecule Crowding Electrolytes for High-Voltage Aqueous Supercapacitors, *ACS Applied Energy Materials*, 2022, **5**, 12067–12077.

20 H. S. Stein, A. Sanin, F. Rahmanian, B. Zhang, M. Vogler, J. K. Flowers, L. Fischer, S. Fuchs, N. Choudhary and L. Schroeder, From materials discovery to system optimization by integrating combinatorial electrochemistry and data science, *Current Opinion in Electrochemistry*, 2022, **35**, 101053.

21 A. Pomberger, N. Jose, D. Walz, J. Meissner, C. Holze, M. Kopczynski, P. Müller-Bischof and A. Lapkin, Automated pH Adjustment Driven by Robotic Workflows and Active Machine Learning, *Chemical Engineering Journal*, 2023, **451**, 139099.

22 *Automation of integrated R&D workflows*, 2022, `https://www.chemspeed.com/integrated-solutions/`.

23 Y. Sui and X. Ji, Anticatalytic Strategies to Suppress Water Electrolysis in Aqueous Batteries, *Chemical Reviews*, 2021, **121**, 6654–6695.

24 K. Xu, Electrolytes and Interphases in Li-Ion Batteries and Beyond, *Chemical Reviews*, 2014, **114**, 11503–11618.

25 Q. Nian, X. Zhang, Y. Feng, S. Liu, T. Sun, S. Zheng, X. Ren, Z. Tao, D. Zhang and J. Chen, Designing Electrolyte Structure to Suppress Hydrogen Evolution Reaction in Aqueous Batteries, *ACS Energy Letters*, 2021, **6**, 2174–2180.

26 F. Häse, L. M. Roch and A. Aspuru-Guzik, Chimera: enabling hierarchy based multi-objective optimization for self-driving laboratories, *Chem. Sci.*, 2018, **9**, 7642–7655.

27 M. Seifrid, R. J. Hickman, A. Aguilar-Granda, C. Lavigne, J. Vestfrid, T. C. Wu, T. Gaudin, E. J. Hopkins and A. Aspuru-Guzik, Routescore: Punching the Ticket to More Efficient Materials Development, *ACS Central Science*, 2022, **8**, 122–131.

28 L. Zhang, X. Hou, K. Edström and E. J. Berg, Reactivity of TiS_2 Anode towards Electrolytes in Aqueous Lithium-Ion Batteries, *Batteries & Supercaps*, e202200336.